Recursive Selective Harmonic Elimination for Multilevel Inverters: Mathematical Formulation and Experimental Validation

Concettina Buccella, *Senior Member, IEEE*, Maria Gabriella Cimoroni, Carlo Cecati, *Fellow, IEEE*, Antonino Oscar Di Tommaso, Rosario Miceli, *Member, IEEE*, Claudio Nevoloso, and Giuseppe Schettino

***Abstract*— A recursive method that eliminates $n+1$ harmonics and their respective multiples from the output voltage of a cascaded H-bridge (CHB) multilevel inverters with $s = 2^n$ dc sources ($n = 1, 2, 3, \ldots$) is proposed. It solves 2×2 linear systems with no singular matrices and always gives an exact solution with very low computational effort. Simulated results in three-phase five-, nine-, 17-, and 33-level CHB inverters, and experimental results in a five-level inverter demonstrate the validity of the method.**

***Index Terms*— Efficiency, modulation, multilevel inverter, selective harmonics elimination (SHE), total harmonic distortion (THD).**

NOMENCLATURE

l	Number of levels.
s	Number of dc voltage sources.
k	Harmonic order.
m	Modulation index.
n	Integer number such that $s = 2^n$.
v_{out}	Output voltage of the multilevel inverter [V].
V	DC voltage feeding each H-bridge [V].
V_{dc}	Rated voltage [V].
V^*	DC voltage feeding each H-bridge [p.u.].
$(4V^*/k\pi)H_k$	kth harmonic amplitude.
α_i, $i = 1, \ldots, s$	Switching angles [rad].
$\alpha_i^{(p)}$, $i = 1, \ldots, s$, $p = n, \ldots, 1$	Intermediate variables (for $p = 1$, $\alpha_i^{(1)} = \alpha_i$).
$(4V^*/k\pi)H_k^{(p)}$	Intermediate variables [for $p = 1$, $(4V^*/k\pi)H_k^{(1)} = (4V^*/k\pi)H_k$].

Manuscript received 14 June 2022; revised 3 September 2022 and 3 November 2022; accepted 5 November 2022. Date of publication 9 November 2022; date of current version 4 April 2023. This work was supported in part by MUR-PRIN 2017 under Project 2017MS9F49; in part by the Sustainable Development and Energy Saving Laboratory (SDESLAB), Laboratory of Electrical Applications (LEAP), Electrical Drive Applications Laboratory (EDALAB), Department of Engineering, University of Palermo, Italy; and in part by DigiPower srl, L'Aquila, Italy. Recommended for publication by Associate Editor Yam Siwakoti. *(Corresponding author: Claudio Nevoloso.)*

Concettina Buccella, Maria Gabriella Cimoroni, and Carlo Cecati are with the Department of Information Engineering, Computer Science and Mathematics, University of L'Aquila, 67100 L'Aquila, Italy, and also with DigiPower srl, 67100 L'Aquila, Italy.

Antonino Oscar Di Tommaso, Rosario Miceli, Claudio Nevoloso, and Giuseppe Schettino are with the Department of Engineering, University of Palermo, 90128 Palermo, Italy (e-mail: claudio.nevoloso@unipa.it).

Color versions of one or more figures in this article are available at https://doi.org/10.1109/JESTPE.2022.3221154.

Digital Object Identifier 10.1109/JESTPE.2022.3221154

I. INTRODUCTION

DUE to their capability to produce approximated sinusoidal output voltages, multilevel inverters are gaining applications in many fields including renewable energy systems, electric traction, industry, and smart grids [1], [2], [3]. The shape of their waveforms gives significant improvements over conventional two-level converters, in terms of lower total harmonics distortion (THD), higher efficiency, increased voltage/power-handling capability, and reduced component stress, hence higher reliability. The main responsible for such features is the adopted modulation technique, which is highly influential both in terms of performance and implementation complexity. Basically, a modulation technique consists of the determination of a set of switching angles, which, then, can be regarded as the unknowns of the modulation problem. Usually, modulation algorithms are classified into three distinct categories: selective harmonic elimination (SHE), selective harmonic mitigation (SHM), and pulsewidth modulation (PWM) algorithms. In general, the first two approaches operate at the fundamental frequency, the latter at high frequency, but, usually, at values significantly lower than in conventional two-level PWM inverters [4], [5], [6], [7], [8], [9], [10]. Since the lower the frequency, the higher the overall efficiency, when possible, that is, in low dynamic systems, it is desirable to adopt SHE or SHM, while multilevel PWM is usually adopted in those applications requiring high bandwidth control. Among the numerous papers on the topic, Sajadi et al. [11] proposed an SHE technique for high-power asymmetrical cascaded H-bridge (CHB) inverters employed for static VAR compensation (STATCOM) application, which is capable to eliminate low-order harmonics, to reduce converter losses, and to regulate the voltage of each dc-link capacitor. To further improve the quality of the output voltages, Buccella et al. [10] proposed to vary the amplitudes of the dc sources, introducing the pulse amplitude width modulation (PAWM), which increases the number of deleted harmonics at

the fundamental switching frequency. Haw et al. [12] proposed a low-switching frequency multilevel SHE-PWM technique for CHB inverters used in transformerless STATCOM systems, which provides constant switching angles and linear pattern dc voltage levels over the full range of the modulation index by employing dc/dc buck converters that operate at a relatively low switching frequency of 2 kHz. Padmanaban et al. [13] proposed an SHE technique for PV systems equipped with a CHB multilevel inverter and boost dc/dc converters, based on an integrated artificial neural network (ANN) and a Newton–Raphson (NR) numerical approach. As discussed in the review paper [14], SHE and SHM modulation techniques are widely used in large electrical drives for traction applications. For instance, Ni et al. [15] proposed a fault-tolerant seven-level CHB motor drive with a nonsymmetrical SHE algorithm that provides a better voltage profile and higher output line voltage amplitude with respect to a conventional frequency phase-shifted compensation approach (FPSC). Steczek et al. [16] proposed to combine SHE and SHM-PWM for railway applications. Schettino et al. [17] used an innovative SHM algorithm in an interior permanent magnet synchronous (IPMSM) drive, obtaining better current THD and drive efficiency than with a conventional multicarrier PWM technique.

This article deals with SHE at a fundamental frequency. In this framework, it is necessary to identify and implement a method capable to find the solutions of the SHE equations or of a nonlinear equations system, corresponding to converter switching angles. In this regard, numerous techniques have been proposed, including iterative approaches [18], optimization methods [19], [20], and mathematical solutions [21], [22]. The first topology presents a set of angles that depends on the initial values, which initially are unknowns and the solution could be divergent. The second topology includes genetic algorithms (GAs), bee algorithms (BAs), and in general artificial intelligence-based algorithms (AGAs) that are not significantly affected by initial values but are complex to implement and present high computational costs [23], [24], [25]. The third typology solves the transcendental equations by algebraic algorithms that are generally computationally efficient. In general, the main drawback is related to the difficulty of solving in real-time the transcendental equations but accurate harmonics cancellation is guaranteed [26], [27]. For instance, Yang et al. [28] proposed an offline computing stage in which the nonlinear equations are linearized by using the theories of symmetric polynomials and Gröbner, then, the linear equations are solved online and their solutions are used to construct a polynomial whose real roots are the switching angles. For CHB five-level inverters, SHE analytical solutions can be obtained in real-time as described in [7] and [8]. Such a method can be extended to a higher number of levels and ensures the elimination of n harmonics.

This work aims to propose a new SHE method for fundamental switching frequency for CHB multilevel inverters, which allows the elimination of more harmonics with respect to the traditional SHE methods. In particular, it allows the elimination of $n+1$ harmonics and their multiples from the output voltage waveform of an l-level CHB inverter with s equal dc sources V depending on modulation index m. The number of voltage levels has to be $l = 2s + 1$, with $s = 2^n$ and $n = 1, 2, 3, \ldots$ The innovation of this procedure is the recursive application of the Prosthaphaeresis formulas that allow obtaining the s switching angles by solving $s - 1$ 2×2 linear system. The modulation index is directly correlated with the amplitude of the dc sources through a proportional coefficient that depends on the eliminated harmonics. In this way, the converter performance in terms of voltage distortion and converter efficiency does not depend on the modulation index.

The main advantages of the proposed procedure are summarized in the following.

1) In inverters with a low number of levels, it returns a higher number of deleted harmonics and a lower THD than the classical SHE technique described in [8].
2) It always returns an analytically exact solution. It is worth to notice that, by using the method proposed in [8], it is not possible to find a solution for all modulation index values and in some cases there are multiple solutions.
3) Being analytical, computational demand is very low, therefore, it could be easily implemented in real-time at low cost [29].
4) The modulation index can be changed in a continuous range from zero to its maximum value.
5) Switching angles and THD do not depend on the modulation index m.
6) The modulation index linearly depends on the dc voltage amplitudes.

This article is structured as follows. Section II presents the mathematical model of a three-phase l-level CHB inverter. Section III describes the proposed method for the elimination of $n+1$ harmonics. Section IV presents the implementation. Section V discusses the computational complexity of the proposed SHE approach. Section VI presents the simulation results obtained with several distinct CHB inverter configurations. Section VII presents the experimental analysis that validates the effectiveness of the proposed method. Section VIII provides a comparison between the proposed SHE approach and other recent methods present in the literature. Finally, Section IX summarizes the key features of the proposed SHE method and reports the study conclusions.

II. Mathematical Model

Fig. 1 shows a three-phase, l-level, CHB inverter. The following constraint is imposed on the number of levels: $l = 2s + 1$, where $s = 2^n$ is the number of dc sources for each phase, with $n = 1, 2, 3, \ldots$ being an integer number. Due to the previous assumption, the proposed procedure can be only used with five-, nine-, 17-, 33-, 65-, or more-level inverters.

The H-bridges are fed by equal dc sources, the amplitudes of which depend on the modulation index m, that is,

$$V_{\mathrm{dc1}}(m) = V_{\mathrm{dc2}}(m) = \cdots = V_{\mathrm{dcs}}(m) = V(m) \tag{1}$$

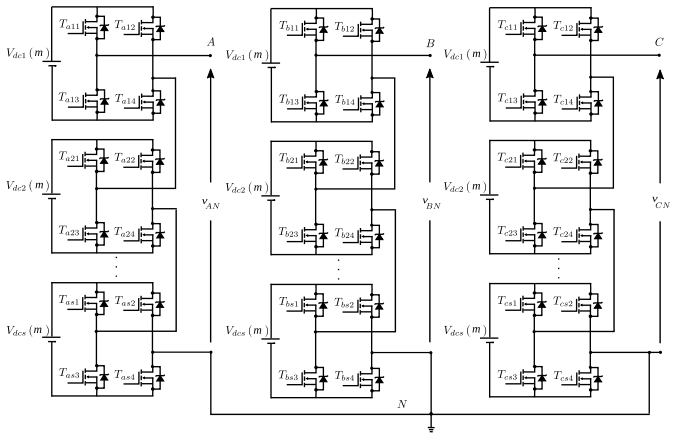

Fig. 1. Three-phase l-level CHB inverter.

whose values in per unit (p.u.) are

$$V^* = \frac{V}{V_{\text{dc}}} = C \cdot m \tag{2}$$

where V_{dc} is the rated voltage, C is a positive coefficient, and m is equal to

$$m = \frac{\pi \widetilde{H}_1}{4s} \tag{3}$$

with $\widetilde{H}_1$ being the amplitude of the fundamental harmonic in p.u. Considering the phase A, the Fourier series of the line-to-neutral output voltage v_{AN} is

$$v_{\text{AN}}(\omega t) = \frac{4}{\pi} \sum_{k=1,3,5,\ldots}^{\infty} \frac{1}{k} V(m) H_k \sin(k\omega t) \tag{4}$$

where

$$H_k = \sum_{i=1}^{s} \cos(k\alpha_i) \tag{5}$$

with α_i being the switching angles with

$$0 < \alpha_i < \frac{\pi}{2}, \quad i = 1, 2, 3, \ldots, s \tag{6}$$

and $\widetilde{H}_k$ is the amplitude of the k-order harmonic, expressed as

$$\widetilde{H}_k = \frac{4}{\pi} \frac{V^*}{k} H_k. \tag{7}$$

From (2), it follows that

$$C = \frac{s}{\sum_{i=1}^{s} \cos(\alpha_i)}. \tag{8}$$

III. Proposed Method

With the previous assumptions, the following mathematical system can be defined to eliminate the $n+1$ harmonics of order $r_1, r_2, \ldots, r_{n+1}$ from the phase voltage of the three-phase l-level CHB inverter

$$\begin{cases} H_{r_1}(\cos(r_1\alpha_1), \ldots, \cos(r_1\alpha_s)) = 0 \\ \vdots \\ H_{r_j}\big(\cos\big(r_j\alpha_1\big), \ldots, \cos\big(r_j\alpha_s\big)\big) = 0 \\ \vdots \\ H_{r_{n+1}}(\cos(r_{n+1}\alpha_1), \ldots, \cos(r_{n+1}\alpha_s)) = 0. \end{cases} \tag{9}$$

In order to calculate the unknowns α_i $i = 1, 2, \ldots, s$ and to solve (9), a recursive procedure can be implemented as described in the following steps.

Step 1: Calling $H_k^{(1)} = H_k$ and $\alpha_i^{(1)} = \alpha_i$, with $i = 1, 2, \ldots, s$, for k that can assume the values $r_1, r_2, \ldots, r_{n+1}$, applying Prosthaphaeresis formulas, it follows that

$$\begin{aligned} H_k^{(1)} &= \sum_{i=1}^{s} \cos\Big(k\alpha_i^{(1)}\Big) = \sum_{i=1}^{s/2} \Big[\cos\Big(k\alpha_{2i-1}^{(1)}\Big) + \cos\Big(k\alpha_{2i}^{(1)}\Big)\Big] \\ &= 2\sum_{i=1}^{s/2} \cos\left(k\frac{\alpha_{2i-1}^{(1)} + \alpha_{2i}^{(1)}}{2}\right) \cos\left(k\frac{\alpha_{2i-1}^{(1)} - \alpha_{2i}^{(1)}}{2}\right). \end{aligned} \tag{10}$$

By (10), the equation $H_{r_1}^{(1)} = 0$ can be satisfied when

$$\frac{\alpha_{2i-1}^{(1)} + \alpha_{2i}^{(1)}}{2} = \frac{\pi}{2r_1}, \quad i = 1, \ldots, \frac{s}{2}. \tag{11}$$

By introducing the new variables $\alpha_i^{(2)} = ((\alpha_{2i-1}^{(1)} - \alpha_{2i}^{(1)})/2)$, $i = 1, \ldots, (s/2)$, the following relations are obtained:

$$\begin{cases} \alpha_{2i-1}^{(1)} + \alpha_{2i}^{(1)} = \dfrac{\pi}{r_1} \\ \alpha_{2i-1}^{(1)} - \alpha_{2i}^{(1)} = 2\alpha_i^{(2)}, \end{cases} \quad i = 1, \ldots, \frac{s}{2}. \tag{12}$$

Substituting (12) in (10), the following expression $H_k^{(1)}$ is obtained:

$$H_k^{(1)} = 2\cos\left(k\frac{\pi}{2r_1}\right) H_k^{(2)} \tag{13}$$

where

$$H_k^{(2)} = \sum_{i=1}^{s/2} \cos\Big(k\alpha_i^{(2)}\Big). \tag{14}$$

It is clear that $H_k^{(1)} = 0$ for each $k = jr_1$, with $j = 1, 3, 5, \ldots$, that is, for all odd multiples of r_1.

Steps from 2 to n: By imposing $H_{r_q}^{(q)} = 0$, $q = 2, \ldots, n$, by applying again Prosthaphaeresis formulas and by introducing the new variables $\alpha_i^{(q+1)} = ((\alpha_{2i-1}^{(q)} - \alpha_{2i}^{(q)})/2)$, $i = 1, \ldots, (s/2^q)$, the following nonsingular systems are obtained:

$$\begin{cases} \alpha_{2i-1}^{(q)} + \alpha_{2i}^{(q)} = \dfrac{\pi}{r_q} \\ \alpha_{2i-1}^{(q)} - \alpha_{2i}^{(q)} = 2\alpha_i^{(q+1)}, \end{cases} \quad i = 1, \ldots, \frac{s}{2^q} \tag{15}$$

and

$$H_k^{(q)} = 2\cos\left(k\frac{\pi}{2r_q}\right) H_k^{(q+1)}, \quad q = 2, \ldots, n \tag{16}$$

where

$$H_k^{(q+1)} = \sum_{i=1}^{s/2^q} \cos\Big(k\alpha_i^{(q+1)}\Big). \tag{17}$$

Also in these cases, $H_k^{(q)} = 0$ for each $k = jr_q$, $j = 1, 3, 5, \ldots$, that is, for all odd multiples of r_q.

Step n + 1: As the last step, by (17), $H_k^{(n+1)} = \cos(k((\alpha_1^{(n)} - \alpha_2^{(n)})/2))$ and imposing $H_{r_{n+1}}^{(n+1)} = 0$ the (15), for $q = n$ becomes

$$\begin{cases} \alpha_1^{(n)} + \alpha_2^{(n)} = \dfrac{\pi}{r_n} \\ \alpha_1^{(n)} - \alpha_2^{(n)} = \dfrac{\pi}{r_{n+1}} \end{cases} \tag{18}$$

therefore, by (13) and (16) follows that

$$H_k^{(1)} = 2^q \prod_{j=1}^{q} \cos\left(k\frac{\pi}{2r_j}\right) H_k^{(q+1)}, \quad q = 1, \ldots, n \tag{19}$$

and for $q = n$, by (18) $H_k^{(n+1)} = \cos(k(\pi/2r_{n+1}))$ and by (19) follows that

$$H_k^{(1)} = 2^n \prod_{j=1}^{n+1} \cos\left(k\frac{\pi}{2r_j}\right). \tag{20}$$

The unknown switching angles $\alpha_i^{(1)} = \alpha_i$ in (12) are computed after solving (18), (15) for $q = 2, \ldots, n-1$ and (12).

IV. Implementation

The proposed recursive method consists of the algorithm shown in the flowchart of Fig. 2. It starts from the solution of (18) and stops with the solutions of the $s/2$th systems in (12).

The algorithm considers the matrix

$$A = \begin{pmatrix} 1 & 1 \\ 1 & -1 \end{pmatrix} \tag{21}$$

its inverse $\boldsymbol{B} = (\mathbf{1}/\mathbf{2})\boldsymbol{A}$ and $r_1, \ldots, r_{n+1}$ with $n \geq 1$ such that $s = 2^n$ and obtains the solution as

$$\begin{pmatrix} \alpha_1^{(n)} \\ \alpha_2^{(n)} \end{pmatrix} = \boldsymbol{B} \begin{pmatrix} \dfrac{\pi}{r_n} \\ \dfrac{\pi}{r_{n+1}} \end{pmatrix}. \tag{22}$$

If $n > 1$, for $p = 1, \ldots, n-1$, 2^p systems are solved as

$$\begin{pmatrix} \alpha_{2i-1}^{(n-p)} \\ \alpha_{2i}^{(n-p)} \end{pmatrix} = B \begin{pmatrix} \dfrac{\pi}{r_{n-p}} \\ 2\alpha_i^{(n-p+1)} \end{pmatrix}, \quad i = 1, \ldots, 2^p. \tag{23}$$

The switching angles (6) are $\alpha_i^{(1)}$ $i = 1, 2, \ldots, s$ and they are obtained by solving (23) when $p = n - 1$.

V. Computational Complexity

In the flowchart in Fig. 2, it is possible to observe that a 2×2 linear system has been solved before entering in the double cycle in p and i. Inside the inner cycle, in the variable i, 2^p linear systems with p in the range $[1, n-1]$ are solved, therefore, the number of solved systems is

$$N_s = 1 + \sum_{p=1}^{n-1} 2^p = \sum_{p=0}^{n-1} 2^p = \frac{2^n - 1}{2 - 1} = 2^n - 1 = s - 1. \tag{24}$$

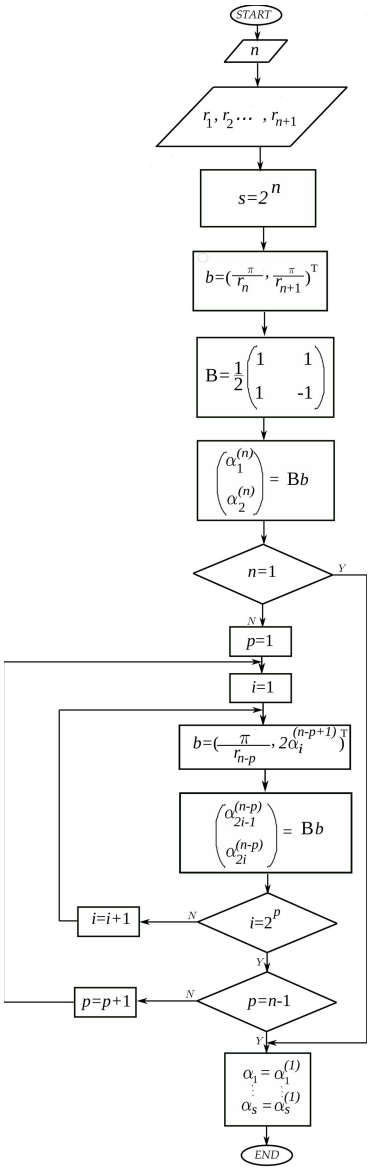

Fig. 2. Flowchart of switching angles computation algorithm.

The computational complexity T_a of the proposed algorithm is

$$T_a = (s - 1)T_{\text{sc}} \tag{25}$$

where T_{sc} is a matrix–vector scalar product with a 2×2 matrix, that is, $T_{\text{sc}} = 2T_{\text{addition}} + 4T_{\text{multiplication}}$ where T_{addition} and $T_{\text{multiplication}}$ are time factors for addition and multiplication operations, respectively.

A. Application of the Method to a Three-Phase Five-Level Inverter

Using a five-level CHB inverter, the proposed method can eliminate two harmonics. This case is particularly simple and its implementation requires very limited effort. In fact, the method is not recursive and the switching angles are computed

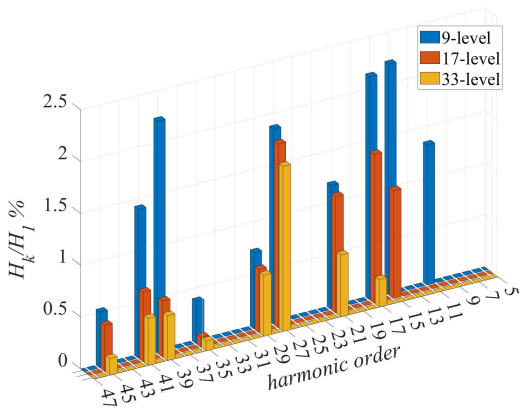

Fig. 3. Comparative phase voltage harmonic analysis.

as follows:

$$\begin{cases} \alpha_1 = \dfrac{\pi}{2}\left(\dfrac{1}{r_1} + \dfrac{1}{r_2}\right) \\ \alpha_2 = \dfrac{\pi}{2}\left(\dfrac{1}{r_1} - \dfrac{1}{r_2}\right) \end{cases} \tag{26}$$

therefore $T_a = 2T_{\text{addition}} + 2T_{\text{multiplication}}$.

B. Comparison With the SHE Algorithm [8]

In [8], the analytical solution, that is, the values of the switching angles, has been found for a five-level CHB inverter, operating at the fundamental frequency, considering the equal and fixed source voltages that do not depend on the modulation index. For a fixed modulation index m, the computational complexity of the modulation algorithm in [8] is

$$T_{a[8]} = (T_{\cos} + T_{\arccos} + 3T_{\text{multiplication}} + 2T_{\text{division}}) \tag{27}$$

where $T_{\cos}$ and $T_{\arccos}$ are time factors of cos function and arccos functions, respectively. Therefore, being $s = 2$, $T_a = T_{\text{sc}} < T_{a[8]}$.

Other methods described in the literature are iterative, therefore, they present poorly predictable and, in general, high computational complexity [4], [30].

VI. Simulated Results

In order to validate the effectiveness of the proposed approach, numerical analysis has been carried out using MATLAB.[1] Figs. 3 and 4 show the phase voltage harmonic analysis and the corresponding THD for a three-phase, nine-, 17-, and 33-level CHB inverter, which can be considered cases of practical interest.

The impact of missing harmonics on the THD can be various, therefore, it is interesting to consider and compare several combinations of eliminated harmonics. Since the prototype available in the Sustainable Development and Energy Saving Laboratory (SDESLAB) of the University of Palermo is a three-phase five-level CHB inverter, this detailed analysis has been restricted to this CHB topology for consequent experimental validation. Five cases have been considered as reported in Table I. Control angles have been evaluated for each case study, and the corresponding modulation index range, expressed in (28) by considering (3) and (5), is reported below

$$m = \frac{V}{V_{\text{dc}}} \cdot [\cos\alpha_1 + \cos\alpha_2]. \tag{28}$$

It must be noted that the expression (28) describes the relation of m interval with the constraint regarding the number of the dc sources and control angles, and consequently with the $n + 1$ eliminated harmonics. Therefore, by fixing n, the value of the modulation index depends only on the dc voltage amplitude. Fig. 5 shows the THD% trend versus modulation index [see Fig. 5(a)] and the low-order harmonics spectra comparison [see Fig. 5(b)] for each case study. In Case 1, the lowest values of THD% have been obtained by eliminating both the 5th and the 11th harmonic, moreover, it can be observed that the THD% values do not depend on the modulation index. In Case 2, by eliminating the fifth and 11th harmonics (orange bar graph), the predominant harmonics are seventh and 19th with an amplitude of about 4%, as shown in Fig. 5(b), where low-order harmonics spectra are compared. Thus, this result explains the lower values of the THD% in this case.

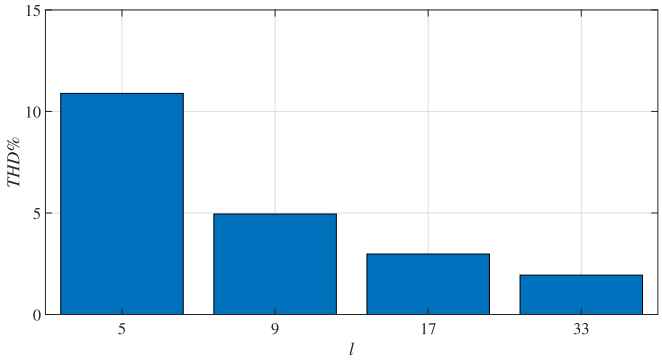

Fig. 4. Phase voltage THD% versus CHB inverter level number (l).

VII. Experimental Results

A test rig, shown in Fig. 6, has been assembled at SDESLab. It is composed of the following.

1) A three-phase five-level CHB MOSFET-based inverter obtained by assembling six distinct H-bridges controlled by a control board employing an Intel-Altera Cyclone III FPGA, programed in VHDL with 32-bit arithmetics. The system is produced by DigiPower and the main technical data are reported in Table II. The power rating of each H-Bridge module is 5 kW, obtaining a 30-kW power rating for a three-phase five-level CHB inverter prototype.
2) Six programmable dc power supplies RSP-2400 whose main technical data are reported in Table III [31].
3) A passive electric load RL (constantan rheostats with $R = 20\ \Omega$ and $L = 10$ mH).
4) A Teledyne LeCroy WaveRunner Oscilloscope 640Zi, two Yokogawa 700 924 differential voltage probes, and two Yokogawa 701 933 current probes.
5) Two Yokogawa power meters (WT 330 and WT 130).

[1]Registered trademark.

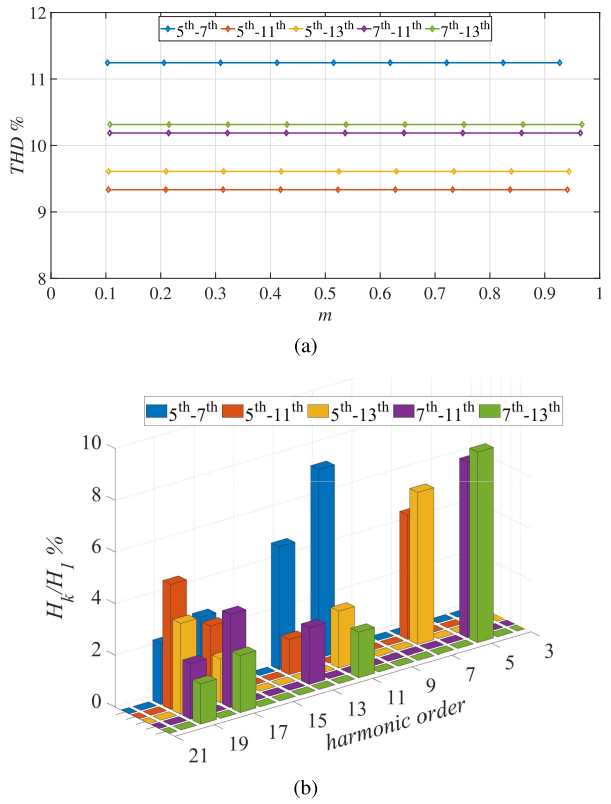

Fig. 5. Simulation analysis of a three-phase five-level CHB inverter. (a) THD% versus modulation index. (b) Harmonics spectra comparison.

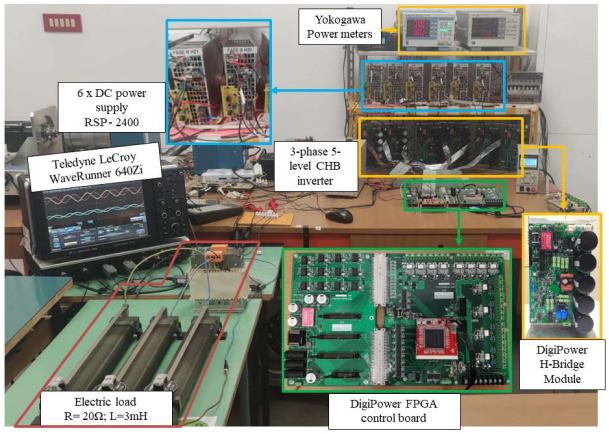

Fig. 6. Test bench.

Fig. 7 shows a schematic representation of the implemented system, including the measurement circuit. The experimental validation was carried out in two steps and the experimental results were compared with those obtained with the SHE algorithm [8]. In the first analysis, load tests with an RL load ($R = 20\ \Omega$ and $L = 10$ mH) were carried out to validate the proposed approach, and the line voltage harmonic content of the proposed algorithm was reported by using the THD% as a comparative parameter at no-load working conditions. After that, the converter efficiency was measured in the cases summarized in Table I and compared with those measured implementing the SHE algorithm discussed in [8].

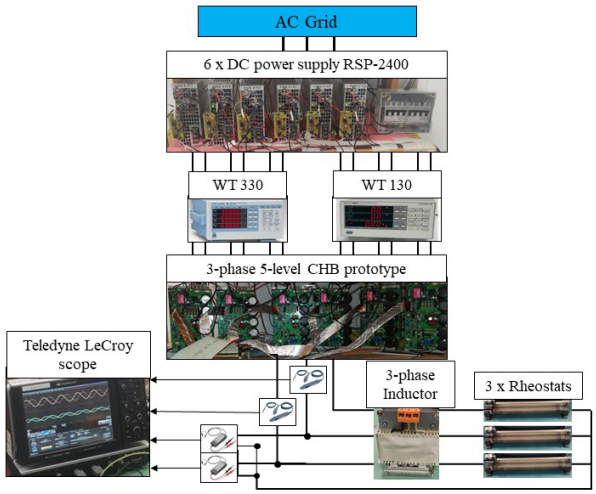

Fig. 7. Schematic representation of the circuit with measurement points.

TABLE I
CASE STUDIES OF THE PROPOSED ALGORITHMS

Case	Eliminated harmonics	Control angles [rad]	Modulation index
1	5^{th} and 7^{th}	$\alpha_1 = 0.5386$ $\alpha_2 = 0.0898$	$0 \leq m \leq 0.9272$
2	5^{th} and 11^{th}	$\alpha_1 = 0.4570$ $\alpha_2 = 0.1714$	$0 \leq m \leq 0.9414$
3	5^{th} and 13^{th}	$\alpha_1 = 0.4350$ $\alpha_2 = 0.1933$	$0 \leq m \leq 0.9441$
4	7^{th} and 11^{th}	$\alpha_1 = 0.3672$ $\alpha_2 = 0.0816$	$0 \leq m \leq 0.9650$
5	7^{th} and 13^{th}	$\alpha_1 = 0.3452$ $\alpha_2 = 0.1036$	$0 \leq m \leq 0.9678$

A. Validation and Converter THD Analysis

In order to demonstrate the effectiveness of the proposed approach, Fig. 8 shows the line voltage (yellow curve), phase current (cyan curve), and corresponding voltage harmonic distribution in the frequency domain (red bar graph) for each analyzed case at dc input voltages equal to 40 V. The voltage, current, and time scales were set to 50 V/div, 2 A/div, and 5 ms/div, respectively; the harmonic spectra in the frequency domain present a voltage scale equal to 20 V/div and a frequency scale equal to 200 Hz/div. As shown in Fig. 8, it should be noted that the selected harmonics were eliminated in each case demonstrating the effectiveness of the proposed algorithm. In order to evaluate dynamic performances during the elimination of pairs of harmonics described in Table I, several tests were carried out for dc voltage steps, corresponding to the modulation index step inside the interval shown in Table I. In this analysis, it is necessary to highlight that the switching angles are constants within all modulation index ranges, resulting in a negligible impact on CHB inverter dynamic performances. Therefore, the CHB inverter transient behavior depends only on the time variation of dc voltage power supplies.

TABLE II
MAIN PARAMETERS OF THE DIGIPOWER CHB INVERTER EMPLOYING MOSFET IRFB4115PBF

Quantity	Symbol	Value
Voltage	$V_{\rm dss}$	150 V
Resistance	R_{DSon}	$9.3\,m\Omega$
Current	I_D	104 A
Turn on delay	T_{Don}	18 ns
Rise time	T_R	73 ns
Turn off delay	T_{Doff}	41 ns
Fall time	T_F	39 ns
Reversal recovery	T_{RR}	86 ns

TABLE III
MAIN DATA OF DC POWER SUPPLY RSP-2400

Section	Quantity	Value
Output	DC Voltage	48 V
	Rated Current	50 A
	Rated Power	2400 W
	Voltage rise time	80 ms (Max) at full load
Input	Voltage range AC	$180-264$ V
	Frequency range	$47-63$ Hz
	Efficiency	91.5%
	AC current	12 A/230 VAC

In order to show the benefit described impact on CHB inverter dynamic performances, the high-side gate signals of each H-bridge module of the same phase, input dc voltages of the same phase, load phase voltage, and phase current were acquired and analyzed. By way of example, Fig. 9 shows high-side gate signals of H-bridge modules (white, purple, orange, and red curves), the load phase voltage (cyan curve), phase current (green curve), and relative input dc voltages (yellow and violet curves) of the CHB inverter when the dc voltage input values change from 20 to 40 V. The corresponding modulation index values were calculated by (28). In detail, Fig. 9(a) and (b) shows the CHB inverter transient behavior with the proposed approach by eliminating fifth and 13th harmonics under modulation index variation from $m = 0.34$ to $m = 0.69$ and eliminating the seventh and the 13th harmonic under modulation index variation from $m = 0.35$ to $m = 0.7$, respectively. It can be noticed that the transient behavior expires after about 50 ms, where the high-side gate signals are not affected by transients, by confirming the negligible impact of the algorithm computation on system dynamic performances. Similar results were obtained for all analyzed cases. The detected dc voltage time transient is attributable to the time constant of the dc power supply only, which is comparable with the rise time reported in the power supply (PSU) datasheet [31]. Fig. 10(a) shows the comparison between experimental and simulation results of THD% versus modulation index for each case analyzed at no load conditions. Moreover, the experimental values of THD% were evaluated for several values of the fundamental frequency. The experimental data confirm the simulation results. In fact, the lowest THD% values were detected in the second case, where the fifth and 11th harmonics were eliminated. Moreover, as expected, no significant THD% variations were detected as the fundamental frequency varies.

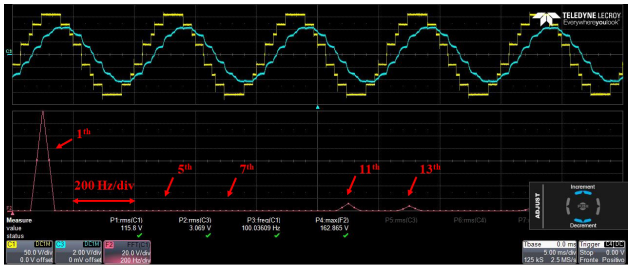

(a)

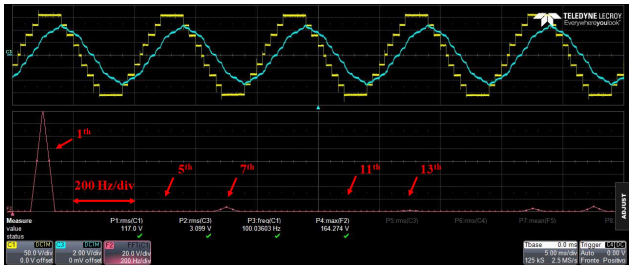

(b)

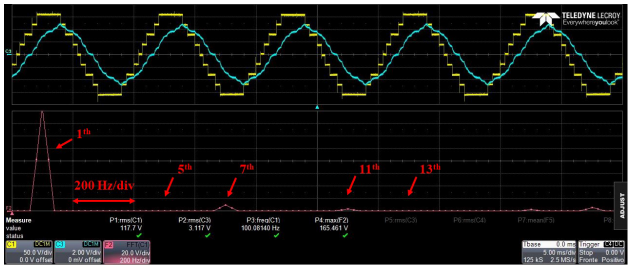

(c)

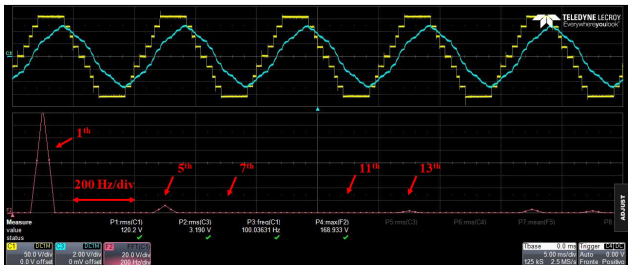

(d)

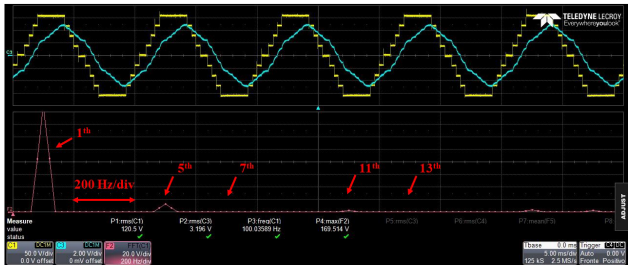

(e)

Fig. 8. CHB inverter experimental results: line voltage (yellow curve), phase current (cyan curve), and voltage harmonic spectra (red bar graph). (a) SHE fifth and seventh—$V = 40$ V. (b) SHE fifth and 11th—$V = 40$ V. (c) SHE fifth and 13th—$V = 40$ V. (d) SHE seventh and 11th—$V = 40$ V. (e) SHE seventh and 13th—$V = 40$ V.

TABLE IV
COMPARISON OF THE PROPOSED SHE APPROACH WITH OTHER SHE APPROACHES

Reference	Harmonics eliminated	Implementation complexity	Modulation index continuity variation	Computational cost	Solution
[8]	n	Low	Yes	Low	exact solution
[29]	$s-1$	High	Yes	High	approximate solution by NR
[20]	$s-1$	High	No	Low	approximate solution by APSO-NR
[13]	$s-1$	High	No	Low	approximate solution by AI
[21]	n and multiples	Low	Yes	Medium	exact solution
Proposed SHE	$n+1$ and multiples	Low	Yes	Low	exact solution

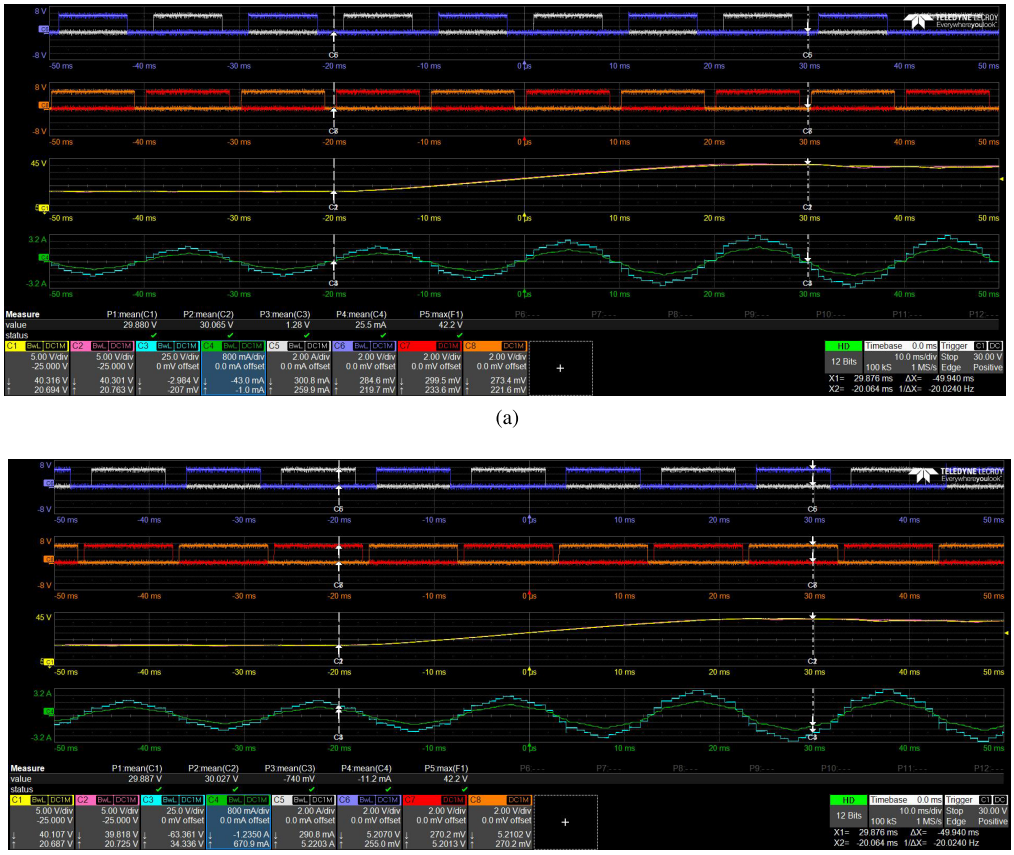

(a)

(b)

Fig. 9. CHB inverter dynamic behavior under dc voltage input change from 20 to 40 V. (a) SHE fifth and 13th with modulation index varying from $m = 0.34$ to $m = 0.69$. (b) SHE seventh and 13th with modulation index varying from $m = 0.35$ to $m = 0.7$.

The proposed approach is suitable in several applications where different fundamental working frequencies are required. In order to demonstrate the improved performance of the proposed algorithm with respect to other traditional SHE algorithms, the experimental THD% values were compared with those obtained by using the SHE algorithm discussed in [8]. In detail, Fig. 10(b) shows that the proposed approach reduces THD% in almost the whole modulation range considered in Table I, with respect to the SHE algorithm proposed in [8] that individually eliminates the fifth, seventh, 11th, and 13th harmonic, respectively. It is worth to notice that comparable results were detected only when the modulation index was around 0.9. Therefore, it is possible to assert that lower values of the THD% were obtained with the proposed algorithm in all cases as shown in Fig. 10(b).

B. Converter Efficiency Analysis

Efficiency is of paramount importance. This section aims to characterize the proposed algorithm in terms of converter

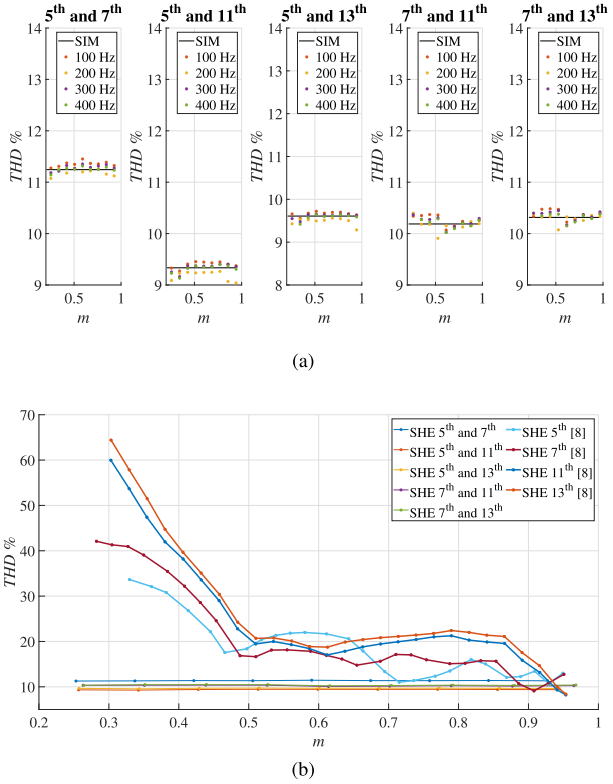

Fig. 10. Experimental comparison of THD% versus modulation index among analyzed cases. (a) Experimental versus simulation results. (b) Proposed algorithm versus SHE in [8].

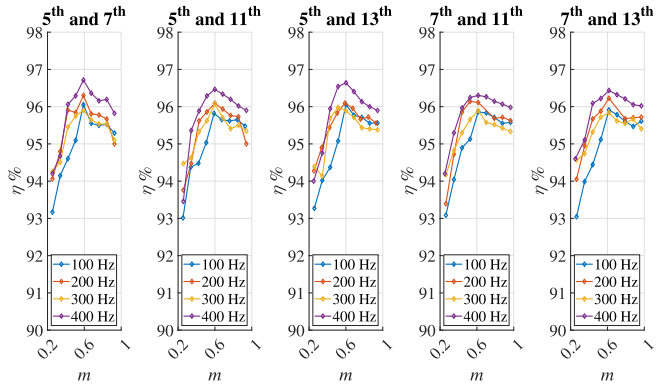

Fig. 11. Experimental converter efficiency versus the modulation index.

efficiency for several values of the modulation index and the fundamental frequency. Moreover, it discusses the input power distribution provided by each dc source, which supplies each H-bridge module. The same working points, analyzed in the no-load tests, were considered for load tests by connecting an electric load with $R = 20\ \Omega$ and $L = 10$ mH. Fig. 11 shows the experimental converter efficiency versus modulation index evaluated for different values of the fundamental frequency from 100 to 400 Hz with 100-Hz steps.

By varying the fundamental frequency, different load displacement power factor (DPF) values—0.95, 0.85, 0.73, and 0.62—were obtained. The efficiency increases as the fundamental frequency increase. This phenomenon can be attributed to the RL load filter effect on the current harmonics. Fig. 12(a) shows converter efficiency versus the modulation

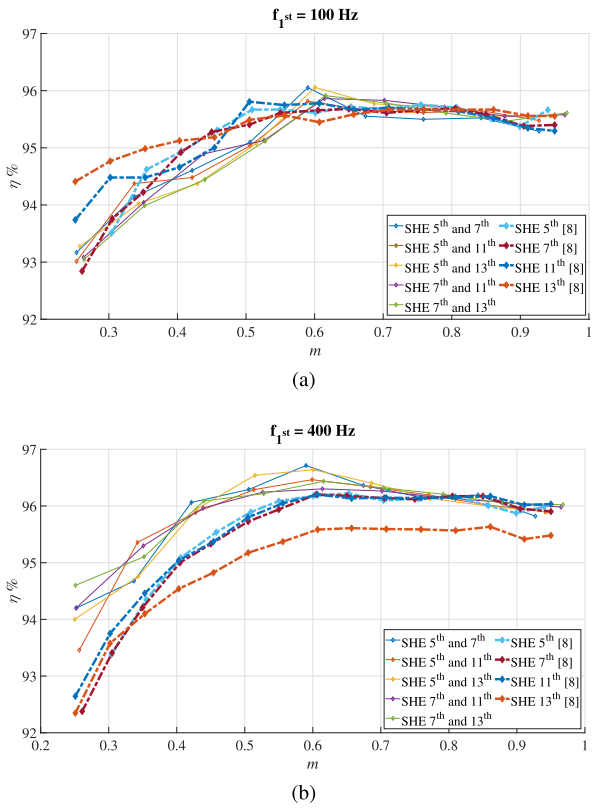

Fig. 12. Experimental converter efficiency versus modulation index compared with respect to SHE algorithm in [8] at different fundamental frequency. (a) 100 Hz. (b) 400 Hz.

index at 100 Hz (DPF = 0.95) obtained with the proposed SHE approach, considering all cases in Table I, and obtained with traditional SHE proposed in [8] eliminating one by one the fifth, the seven7th, the 11th, and the 13th harmonics. Instead, Fig. 12(b) shows the same comparison of converter efficiency as in Fig. 12(a) but at a fundamental frequency equal to 400 Hz (DPF = 0.62), typical of avionics. It is worth to observe that, in all considered cases, converter efficiency is higher than with method [8], in particular, at lower values of the modulation index, which means better control characteristics, especially for the 13th harmonic case and for all considered modulation index values.

Another interesting consideration is the dc power distribution between the H-Bridge modules $P_{\mathrm{HB}i}$ as a function of the modulation index. Fig. 13 shows $P_{\mathrm{HB}i}$ between two H-Bridge modules of the same phase, in percent with respect to the total input power $P_{\mathrm{dc}\,j}$ $(j = A, B, C)$ of the same phase for the proposed approach [see Fig. 13(a)] and for SHE proposed in [8] [see Fig. 13(b)]: the proposed algorithm returns a uniform dc power distribution, which is not the case of [8]. In summary, the analysis carried out and results obtained validate the effectiveness of the proposed SHE approach and highlight better performances with respect to the SHE approach proposed in [8].

VIII. Comparison With Other SHE Algorithms

In order to highlight the main benefits of the proposed SHE approach, a comparative analysis with other recent SHE

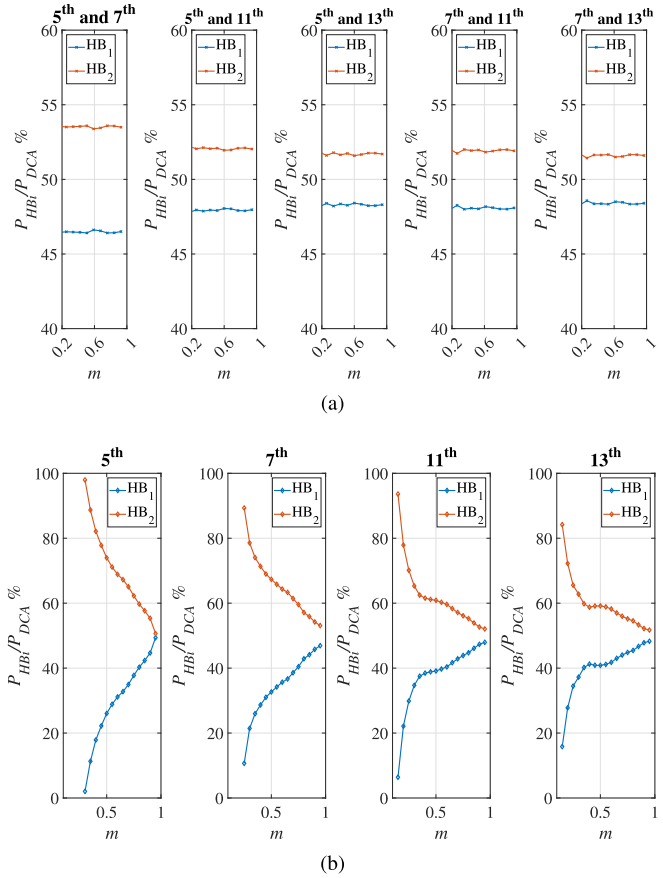

Fig. 13. Experimental dc power distribution. (a) Proposed algorithm. (b) SHE algorithm in [8].

approaches described in [13], [20], [21], and [29] has been carried out by considering as evaluation parameters the number and the order of eliminated harmonics, the implementation complexity, the capability to operate with continuity in a wide modulation index range, the computational cost, and the solution employed. The results of such analysis are summarized in Table IV. Ahmed et al. [29] proposed a real-time solution for the determination of switching angles by using a proportional-integral (PI) controller which is based on the definition of an initial guess. The determination of the switching angles, which are suitable only for fundamental low-frequency applications, guarantees low-order harmonics elimination within the whole modulation index range and the elimination of $s-1$ harmonics. Nevertheless, this approach requires a significant amount of computational time and it does not consider high fundamental frequency analyses. Memon et al. [20] proposed an SHE approach based on hybrid asynchronous particle swarm optimization (APSO) NR algorithm. According to the authors, it provides efficient and accurate identification of the switching angles and fewer iterations than other genetic, Bee and PSO algorithms. However, although it requires just few iterations, its implementation is complex, the number of harmonics eliminated is equal to $s-1$, and it does not guarantee results for the whole modulation index range. Padmanaban et al. [13] proposed a hybrid ANN-NR based on an SHE

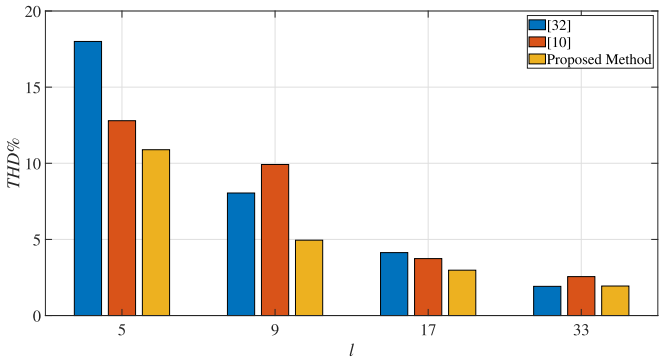

Fig. 14. Comparison among phase voltage THD% obtained with the proposed approach and the considered ML-SHE-PAM and SHE-PAWM approaches.

procedure and suitable for CHB inverters for PV applications. Such an approach employs an ANN for the offline estimation of the switching angles that are used as initial guesses for the NR method. Since it requires just few iterations for optimal identification of the switching angles, it ensures quick convergence, however, it eliminates $s-1$ low-order harmonics but only within a modulation index range [0.68, 0.72]. Although the authors estimate its power losses and efficiency, no comparative analysis with other methods is reported. Finally, Ahmed et al. [21] proposed an interesting general mathematical solution for SHE purposes valid for both symmetrical and asymmetrical CHB inverter configurations. The approach eliminates the targeted harmonics in a wide range of modulation indices and, in asymmetrical CHB configurations, guarantees the cancellation of a larger number of harmonics, but at the cost of higher implementation complexity. Its computation cost increases with the number of eliminated harmonics, and its THD is a function of the modulation index value. For symmetrical multilevel inverter configurations, eliminated harmonics are equal to n and multiples. It is worth noticing that all previously considered papers do not include either a detailed efficiency analysis or the dc power distribution among the H-Bridge modules as well.

To compare THD, the methods proposed in [32] and [10] were implemented and analyzed. The first method, the so-called middle-level SHE pulse amplitude modulation (ML-SHE-PAM), does not delete the harmonics having order $2(l-1)z\pm1$, the second one, the SHE PAWM (SHE-PAWM), does not delete the harmonics having order $2lz\pm1$ with $z=1,2,\ldots$ Fig. 14 shows a comparison among the phase voltage THD% obtained with the proposed approach and ML-SHE-PAM and SHE-PAWM approaches considering up to 301th harmonic. The proposed method offers better performances with CHB inverters with few levels, whereas its performances are comparable in the case of 33-level CHB inverters. Hence, the proposed method outperforms the other methods in cases of more practical interest.

IX. Conclusion

In this article, a new SHE algorithm based on a recursive application of the Prosthaphaeresis formulas has been proposed for the elimination of $n+1$ harmonics and their

multiples from the output voltage waveform of an l-level CHB inverter with s equal dc sources $V(m)$. The proposed approach has been numerically evaluated for different CHB inverter configurations and experimentally validated with a three-phase five-level CHB inverter. Several tests with or without load and considering several case studies confirm that the proposed approach is very effective. Comparisons with the modulation described in [8] highlight much improved performance and lower computational effort. Overall efficiency improves increasing frequency, which makes it suitable for variable speed electrical drives. Moreover, a comparison with some recent SHE approaches described in the literature is reported to highlight the main benefits of the proposed approach. The algorithm can be useful in multilevel photovoltaic inverters, too, taking benefit from dc–dc stages used in maximum power point tracking.

REFERENCES

[1] M. S. A. Dahidah, G. Konstantinou, and V. G. Agelidis, "A review of multilevel selective harmonic elimination PWM: Formulations, solving algorithms, implementation and applications," *IEEE Trans. Power Electron.*, vol. 30, no. 8, pp. 4091–4106, Aug. 2015.

[2] M. Trabelsi, H. Vahedi, and H. Abu-Rub, "Review on single-DC-source multilevel inverters: Topologies, challenges, industrial applications, and recommendations," *IEEE Open J. Ind. Electron. Soc.*, vol. 2, pp. 112–127, 2021.

[3] A. I. Elsanabary, G. Konstantinou, S. Mekhilef, C. D. Townsend, M. Seyedmahmoudian, and A. Stojcevski, "Medium voltage large-scale grid-connected photovoltaic systems using cascaded H-Bridge and modular multilevel converters: A review," *IEEE Access*, vol. 8, pp. 223686–223699, 2020.

[4] S. S. Lee, B. Chu, N. R. N. Idris, H. H. Goh, and Y. E. Heng, "Switched-battery boost-multilevel inverter with GA optimized SHEPWM for standalone application," *IEEE Trans. Ind. Electron.*, vol. 63, no. 4, pp. 2133–2142, Apr. 2016.

[5] J. He, Q. Li, C. Zhang, J. Han, and C. Wang, "Quasi-selective harmonic elimination (Q-SHE) modulation-based DC current balancing method for parallel current source converters," *IEEE Trans. Pow. Electron.*, vol. 34, no. 8, pp. 8201–8212, Aug. 2019.

[6] H. Zhao, S. Wang, and A. Moeini, "Critical parameter design for a cascaded H-Bridge with selective harmonic elimination/compensation based on harmonic envelope analysis for single-phase systems," *IEEE Trans. Ind. Electron.*, vol. 66, no. 4, pp. 2914–2925, Apr. 2019.

[7] C. Buccella, C. Cecati, M. G. Cimoroni, and K. Razi, "Analytical method for pattern generation in five-level cascaded H-Bridge inverter using selective harmonic elimination," *IEEE Trans. Ind. Electron.*, vol. 61, no. 11, pp. 5811–5819, Nov. 2014.

[8] C. Buccella, C. Cecati, M. G. Cimoroni, G. Kulothungan, A. Edpuganti, and A. K. Rathore, "A selective harmonic elimination method for five-level converters for distributed generation," *IEEE J. Emerg. Sel. Topics Power Electron.*, vol. 5, no. 2, pp. 775–783, Jun. 2017.

[9] G. Schettino, F. Viola, A. O. Di Tommaso, P. Livreri, and R. Miceli, "Experimental validation of a novel method for harmonic mitigation for a three-phase five-level cascaded H-Bridges inverter," *IEEE Trans. Ind. Appl.*, vol. 55, no. 6, pp. 6089–6101, Nov. 2019.

[10] C. Buccella, M. G. Cimoroni, M. Tinari, and C. Cecati, "A new pulse active width modulation for multilevel converters," *IEEE Trans. Power Electron.*, vol. 34, no. 8, pp. 7221–7229, Aug. 2019.

[11] R. Sajadi, H. Iman-Eini, M. K. Bakhshizadeh, Y. Neyshabouri, and S. Farhangi, "Selective harmonic elimination technique with control of capacitive DC-link voltages in an asymmetric cascaded H-Bridge inverter for STATCOM application," *IEEE Trans. Ind. Electron.*, vol. 65, no. 11, pp. 8788–8796, Nov. 2018.

[12] L. K. Haw, M. S. A. Dahidah, and H. A. F. Almurib, "SHE–PWM cascaded multilevel inverter with adjustable DC voltage levels control for STATCOM applications," *IEEE Trans. Power Electron.*, vol. 29, no. 12, pp. 6433–6444, Dec. 2014.

[13] S. Padmanaban, C. Dhanamjayulu, and B. Khan, "Artificial neural network and Newton Raphson (ANN-NR) algorithm based selective harmonic elimination in cascaded multilevel inverter for PV applications," *IEEE Access*, vol. 9, pp. 75058–75070, 2021.

[14] A. Poorfakhraei, M. Narimani, and A. Emadi, "A review of modulation and control techniques for multilevel inverters in traction applications," *IEEE Access*, vol. 9, pp. 24187–24204, 2021.

[15] Z. Ni, A. H. Abuelnaga, and M. Narimani, "A new fault-tolerant technique based on nonsymmetrical selective harmonic elimination for cascaded H-Bridge motor drives," *IEEE Trans. Ind. Electron.*, vol. 68, no. 6, pp. 4610–4622, Jun. 2021.

[16] M. Steczek, P. Chudzik, and A. Szelag, "Combination of SHE- and SHM-PWM techniques for VSI DC-link current harmonics control in railway applications," *IEEE Trans. Ind. Electron.*, vol. 64, no. 10, pp. 7666–7678, Oct. 2017.

[17] G. Schettino, C. Nevoloso, R. Miceli, A. O. D. Tommaso, and F. Viola, "Impact evaluation of innovative selective harmonic mitigation algorithm for cascaded H-Bridge inverter on IPMSM drive application," *IEEE Open J. Ind. Appl.*, vol. 2, pp. 347–365, 2021.

[18] W. M. Fei, Y. L. Zhang, and X. B. Ruan, "Solving the SHEPWM nonlinear equations for three-level voltage inverter based on computed initial values," in *Proc. IEEE Appl. Power Electron. Conf.*, Feb. 2007, pp. 1084–1088.

[19] K. Haghdar, "Optimal DC source influence on selective harmonic elimination in multilevel inverters using teaching–learning-based optimization," *IEEE Trans. Ind. Electron.*, vol. 67, no. 2, pp. 942–949, Feb. 2020.

[20] M. A. Memon, S. Mekhilef, and M. Mubin, "Selective harmonic elimination in multilevel inverter using hybrid APSO algorithm," *IET Power Electron.*, vol. 11, no. 10, pp. 1673–1680, Aug. 2018.

[21] M. Ahmed et al., "General mathematical solution for selective harmonic elimination," *IEEE J. Emerg. Sel. Topics Power Electron.*, vol. 8, no. 4, pp. 4440–4456, Dec. 2020.

[22] K. Yang et al., "Unified selective harmonic elimination for multilevel converters," *IEEE Trans. Power Electron.*, vol. 32, no. 2, pp. 1579–1590, Feb. 2017.

[23] A. Routray, R. K. Singh, and R. Mahanty, "Harmonic minimization in three-phase hybrid cascaded multilevel inverter using modified particle swarm optimization," *IEEE Trans. Ind. Informat.*, vol. 15, no. 8, pp. 4407–4417, Aug. 2019.

[24] A. Kavousi, B. Vahidi, R. Salehi, M. K. Bakhshizadeh, N. Farokhnia, and S. H. Fathi, "Application of the bee algorithm for selective harmonic elimination strategy in multilevel inverters," *IEEE Trans. Power Electron.*, vol. 27, no. 4, pp. 1689–1696, Apr. 2012.

[25] F. Filho, H. Z. Maia, T. H. A. Mateus, B. Ozpineci, L. M. Tolbert, and J. O. P. Pinto, "Adaptive selective harmonic minimization based on ANNs for cascade multilevel inverters with varying DC sources," *IEEE Trans. Ind. Electron.*, vol. 60, no. 5, pp. 1955–1962, May 2013.

[26] Z. Yuan, R. Yuan, W. Yu, J. Yuan, and J. Wang, "A Groebner bases theory-based method for selective harmonic elimination," *IEEE Trans. Power Electron.*, vol. 30, no. 12, pp. 6581–6592, Dec. 2015.

[27] H. Zhao, T. Jin, S. Wang, and L. Sun, "A real-time selective harmonic elimination based on a transient-free inner closed-loop control for cascaded multilevel inverters," *IEEE Trans. Power Electron.*, vol. 31, no. 2, pp. 1000–1014, Feb. 2016, doi: 10.1109/TPEL.2015.2413898.

[28] K. Yang et al., "Real-time switching angle computation for selective harmonic control," *IEEE Trans. Power Electron.*, vol. 34, no. 8, pp. 8201–8212, Aug. 2019.

[29] M. Ahmed, A. Sheir, and M. Orabi, "Real-time solution and implementation of selective harmonic elimination of seven-level multilevel inverter," *IEEE J. Emerg. Sel. Topics Power Electron.*, vol. 5, no. 4, pp. 1700–1709, Dec. 2017.

[30] M. H. Etesami, D. M. Vilathgamuwa, N. Ghasemi, and D. P. Jovanovic, "Enhanced metaheuristic methods for selective harmonic elimination technique," *IEEE Trans. Ind. Informat.*, vol. 14, no. 12, pp. 5210–5220, Dec. 2018.

[31] [Online]. Available: https://www.meanwell.com/Upload/PDF/RSP-2400/RSP-2400-SPEC.PDF

[32] P. L. Kamani and M. A. Mulla, "Middle-level SHE pulse-amplitude modulation for cascaded multilevel inverters," *IEEE Trans. Ind. Electron.*, vol. 65, no. 3, pp. 2828–2833, Mar. 2018.

Concettina Buccella (Senior Member, IEEE) received the M.Sc. degree from the University of L'Aquila, L'Aquila, Italy, in 1988, and the Ph.D. degree in electrical engineering from the University of Rome "La Sapienza," Rome, Italy, in 1995.

From 1988 to 1989, she was a Research and Development Engineer with Italtel SpA, L'Aquila. She joined the Department of Electrical Engineering, University of L'Aquila, in 1991, where she is currently a Professor of power converters, electric machines, and drives and the Chair of B.Sc. in ICT engineering. She is the Chief Scientific Officer with DigiPower Ltd., L'Aquila, a research and development company active in the field of power electronics. Her research interests include power converters modulation techniques, renewable energy, smart grids, and analytical and numerical modeling of electric systems.

Dr. Buccella was a co-recipient of the 2012 and 2013 Best Paper Award of the IEEE TRANSACTIONS ON INDUSTRIAL INFORMATICS. From 2017 to 2018, she was the Chair of the IEEE-IES Technical Committee on Renewable Energy Systems. She has been an Associate Editor of the IEEE TRANSACTIONS ON INDUSTRIAL ELECTRONICS and the IEEE SYSTEMS JOURNAL.

Maria Gabriella Cimoroni received the M.Sc. degree *(summa cum laude)* in mathematics from the University of L'Aquila, L'Aquila, Italy, in 1989.

After graduation, she attended the postgraduate Inter-University School, Perugia, Italy, and the CNR Computational Mathematics School, Naples, Italy. Since 1994, she has been a Researcher in numerical analysis with the University of L'Aquila. Her research activities deal with new spline operators for the approximation of functions, for numerical evaluation of Cauchy principal value integrals, and for the numerical solution of integro-differential equations, and since some years with analytical and numerical methods for modulation algorithms for multilevel converters.

Prof. Cimoroni has been a reviewer for several international conferences and IEEE TRANSACTIONS. She was the Publication Chair for the IEEE IECON 2016 and the Publicity Chair for the 5th International Symposium on Environment Friendly Energies and Application 2018 in Rome.

Carlo Cecati (Fellow, IEEE) received the Dr.Ing. degree in electrotechnical engineering from the University of L'Aquila, L'Aquila, Italy, in 1983.

Since 1983, he has been with the University of L'Aquila, where he has also been a Professor of industrial electronics and drives since 2006. From 2015 to 2017, he was a Qianren Talents Professor with the Harbin Institute of Technology, Harbin, China. He is the Chief Technical Officer at DigiPower Ltd., L'Aquila, a research and development company active in the field of power electronics. His primary research interests include power electronics, distributed generation, e-transportation, and smart grids.

Dr. Cecati was a co-recipient of the 2012 and 2013 Best Paper Award from the IEEE TRANSACTIONS ON INDUSTRIAL INFORMATICS, the 2012 Best Paper Award from the *IEEE Industrial Electronics Magazine*, and the 2019 Outstanding Paper Award from the IEEE TRANSACTIONS ON INDUSTRIAL ELECTRONICS. In 2017, he received the Antony J. Hornfeck Award from the IEEE Industrial Electronics Society. In 2019, he received the title of "Commander of the Republic of Italy" from the President of the Republic of Italy. In 2021, he received the Eugene Mittlemann Achievement Award from the IEEE. He was the Coeditor-in-Chief from 2010 to 2012 and the Editor-in-Chief from 2013 to 2015 of the IEEE TRANSACTIONS ON INDUSTRIAL ELECTRONICS.

Antonino Oscar Di Tommaso was born in Tübingen, Germany, on June 5, 1972. He received the master's and Ph.D. degrees in electrical engineering from the University of Palermo, Palermo, Italy, in 1999 and 2004, respectively.

He was a Post Ph.D. Fellow of electrical machines and drives, from 2004 to 2006, and a Researcher, from 2006 to 2019, with the Department of Electrical Engineering, University of Palermo, where he is currently an Associate Professor of electrical machines and drives with the Department of Engineering. His research interests include electrical machines, drives, diagnostics on power converters, and diagnostics and design of electrical machines.

Rosario Miceli (Member, IEEE) received the B.S. and Ph.D. degrees in electrical engineering from the University of Palermo, Palermo, Italy, in 1982 and 1987, respectively.

He is currently a Full Professor of electrical machines with the Polytechnic School, University of Palermo, where he is also a Personnel in Charge with the Sustainable Development and Energy Savings Laboratory. His main research interests include mathematical models of electrical machines, drive system control and diagnostics, renewable energies, and energy management.

Dr. Miceli is a Reviewer of the IEEE TRANSACTIONS ON INDUSTRIAL ELECTRONICS and the IEEE TRANSACTIONS ON INDUSTRY APPLICATIONS.

Claudio Nevoloso received the M.S. and Ph.D. degrees in electrical engineering from the University of Palermo, Palermo, Italy, in 2016 and 2020, respectively.

He is currently a Post-Doctoral Researcher with the Sustainable Development and Energy Saving Laboratory, University of Palermo, where he works on advanced control and characterization of electrical drives. His main research interests include the design, mathematical modeling, control, and characterization of electrical machines, implementation of modulation strategies, and control techniques for electric drives fed by multilevel power converters.

Giuseppe Schettino received the bachelor's and master's degrees in electrical engineering and the Ph.D. degree in energy and information technologies from the University of Palermo, Palermo, Italy, in 2012, 2015, and 2018, respectively, with the Ph.D. thesis "Cascaded H-Bridges multilevel inverter: grid connected advanced applications."

He is currently a Post-Doctoral Researcher with the Department of Engineering, University of Palermo. He has coauthored more than 65 papers published in international conference proceedings and journals. His research interests include multilevel power converters, modulation techniques, and control strategies for grid-connected and electrical drive applications.

Open Access funding provided by 'Università degli Studi di Palermo' within the CRUI CARE Agreement